

Institut für Veterinärpathologie  
der Vetsuisse-Fakultät Universität Zürich

Direktorin: Prof. Dr. med. vet. Anja Kipar

Arbeit unter wissenschaftlicher Betreuung von  
Prof. Dr. med. vet. Anja Kipar

**Feline Hypertrophic Cardiomyopathy, the Consequence of Cardiomyocyte Initiated  
and Macrophage Driven Remodeling Processes?**

**Inaugural-Dissertation**

zur Erlangung der Doktorwürde der  
Vetsuisse-Fakultät Universität Zürich

vorgelegt von

**Sarah Verena Kitz**

Tierärztin  
aus Wien, Österreich

genehmigt auf Antrag von

Prof. Dr. med. vet. Anja Kipar, Referentin  
Prof. Dr. med. vet. Tony Glaus, Korreferent

**2018**

## Inhaltsverzeichnis

Abstract.....	4
Zusammenfassung.....	5
Original Article.....	6
Abstract.....	7
Introduction.....	8
Material and Methods.....	9
Results.....	14
Discussion.....	19
Acknowledgements.....	24
References .....	25
Supplements.....	30

Vetsuisse Faculty University of Zurich

2018 Sarah Verena Kitz

Institute of Veterinary Pathology  
ivpz@vetpath.uzh.ch

## Feline Hypertrophic Cardiomyopathy, the Consequence of Cardiomyocyte Initiated and Macrophage Driven Remodeling Processes?

Hypertrophic cardiomyopathy is the most commonly diagnosed cardiac disease in cats. Its complex pathophysiology is still not clear, but myocardial remodelling is a key process, and cardiomyocyte disarray, interstitial fibrosis, leukocyte infiltration and vascular dysplasia are described histopathologic features.

The present systematic pathological study aimed to shed more light on the pathogenesis of HCM.

Hearts from each 18 HCM and control cases were examined, using light and transmission electron microscopy, immunohistochemistry and morphometric approaches to identify and quantify the morphological changes. Quantitative reverse transcriptase PCR served to gain mechanistic data on remodelling processes. In HCM, the left and right ventricular free wall and septal myocardium exhibited a significantly reduced overall cellularity, accompanied by a significant increase in interstitial Iba1-positive cells with macrophage morphology. In addition, the myocardium of almost half of the diseased hearts exhibited areas where cardiomyocytes were replaced by cell rich fibrous tissue with abundant small and medium sized vessels. HCM hearts also showed significantly higher transcription levels for several inflammatory and profibrotic mediators.

The results suggest that HCM is the consequence of cardiac remodeling processes that are the result of cardiomyocyte damage and to which macrophages contribute by maintaining an inflammatory and profibrotic environment.

Keywords: cat, heart, hypertrophic cardiomyopathy, morphometry, myocardium, histopathology

Sarah Verena Kitz

Institut für  
Veterinärpathologie  
ivpz@vetpath.uzh.ch

Feline Hypertrophe Kardiomyopathie, die Konsequenz eines von Kardiomyozyten initiierten und Makrophagen gesteuerten Umbauprozesses?

Hypertrophe Kardiomyopathie (HCM) ist die häufigste diagnostizierte Herzerkrankung bei Katzen. Ihre komplexe Pathophysiologie ist noch unklar, aber myokardialer Umbau ist ein Hauptprozess und kardiomyozytärer 'Disarray', interstitielle Fibrose, leukozytäre Infiltrate und vaskuläre Dysplasien sind beschriebene histologische Merkmale. Die vorliegende systematische pathologische Studie diente dazu, mehr Klarheit zur Pathogenese der HCM zu erlangen. Herzen von 18 HCM-Fällen und Kontrollkatzen wurden mittels Lichtmikroskopie einschliesslich Immunhistochemie und morphometrischen Ansätzen sowie Transmissionselektronenmikroskopie untersucht, um die morphologischen Veränderungen zu identifizieren und zu quantifizieren. Mittels RT-PCR wurden Daten zu Umbaumechanismen gewonnen. Bei HCM wies das Myokard der linken und rechten Ventrikelwand und des Septums eine signifikant reduzierte Zellzahl, sowie signifikant mehr interstitielle Iba-1-positiven Zellen (Makrophagen) auf. Bei nahezu der Hälfte der Fälle fanden sich Herde, in denen das Myokardium durch zellreiches fibrovaskuläres Gewebe ersetzt war. Ausserdem war die HCM mit einer signifikant erhöhten Transkription einiger Entzündungs- und profibrotischer Mediatoren verbunden. Die Ergebnisse weisen darauf hin, dass die feline HCM Folge kardialer Umbauprozesse ist, die sich infolge Kardiomyozytenschädigung und durch Makrophagen aufrechterhaltene entzündliche und profibrotische Prozesse entwickelt.

Stichwörter: Katze, Herz, Hypertrophe Kardiomyopathie, Morphometrie, Myokardium, Histopathologie

## **Original Article**

# **Feline Hypertrophic Cardiomyopathy, the Consequence of Cardiomyocyte Initiated and Macrophage Driven Remodeling Processes?**

**S. Kitz<sup>1</sup>, S. Fonfara<sup>2</sup>, S. Hahn<sup>3,\*</sup>, U. Hetzel<sup>1</sup>, A. Kipar<sup>1</sup>**

The Veterinary Cardiac Pathophysiology Consortium

<sup>1</sup>Institute of Veterinary Pathology, Vetsuisse Faculty, University of Zurich, Switzerland; <sup>2</sup>Department of Clinical Studies, Ontario Veterinary College, University of Guelph, Canada; <sup>3</sup>Department of Basic Veterinary Sciences, Faculty of Veterinary Medicine, University of Helsinki, Finland

\*Author's current address: Kimron Veterinary Institute, Bet Dagan, Israel

### **Corresponding author:**

Anja Kipar  
Institute of Veterinary Pathology  
Vetsuisse Faculty  
University of Zurich  
Winterthurerstrasse 268  
CH - 8057 Zurich  
Switzerland  
E-mail: [anja.kipar@uzh.ch](mailto:anja.kipar@uzh.ch)

## **Abstract**

Hypertrophic cardiomyopathy (HCM) is the most commonly diagnosed cardiac disease in cats. The complex pathophysiology of HCM is still far from clear, but myocardial remodeling is a key process, and cardiomyocyte disarray, interstitial fibrosis, leukocyte infiltration and vascular dysplasia are described histopathologic features. The present study systematically investigated the pathological processes in HCM, with the aim to shed more light on its pathogenesis. Hearts from 18 HCM cases and 18 cats without cardiac disease (controls) were examined, using light and transmission electron microscopy, immunohistochemistry and morphometric approaches to identify and quantify the morphological changes. Quantitative reverse transcriptase PCR was applied to provide additional mechanistic data on remodeling processes. In HCM, the left and right ventricular free wall and septal myocardium exhibited a significantly reduced overall cellularity, accompanied by a significant increase in interstitial Iba1-positive cells with macrophage morphology. In addition, the myocardium of almost half of the diseased hearts exhibited areas where cardiomyocytes were replaced by cell rich fibrous tissue with abundant small and medium sized vessels. HCM hearts also showed significantly higher transcription levels for several inflammatory and profibrotic mediators. Our results suggest that HCM is the consequence of cardiac remodeling processes that are the result of cardiomyocyte damage and to which macrophages contribute by maintaining an inflammatory and profibrotic environment.

**Keywords:** cat, heart, hypertrophic cardiomyopathy, morphometry, myocardium, histopathology

Feline hypertrophic cardiomyopathy (HCM) is defined by an unexplained thickening of the left ventricular wall without dilation of the chambers and in absence of any other cardiac or non-cardiac disease that itself is capable of causing hypertrophy of the heart.<sup>28,29,31</sup> HCM is the most commonly diagnosed cardiac disease in cats.<sup>8,29,31</sup> It is a heterogeneous disease, both in its clinical presentation and progression.<sup>1</sup> A retrospective study has shown a familial predisposition in Persian, American Shorthair, Maine Coon and Ragdoll cats.<sup>8</sup> In Maine Coon and Ragdolls, HCM has been linked to mutations in a sarcomeric gene.<sup>23,24</sup> Epidemiological studies have shown a sex predisposition for male cats and a mean age of 6 years at the time of diagnosis.<sup>1,28,29</sup> Affected cats can present with signs of congestive heart failure (CHF) and arterial thromboembolism (AT), or can suffer sudden death, though many never exhibit any clinical signs of cardiac disease and die of non-cardiac conditions.<sup>4,28,32</sup>

To the authors' knowledge, the first study on feline primary myocardial disease and CHF was published in 1970; this and subsequent papers reported a range of pathological features for HCM.<sup>2,3,12,17,20</sup> Macroscopically, feline HCM is characterised by a concentric symmetrical (generalised) or asymmetrical (focal) thickening of the interventricular septum, left ventricle, and the papillary muscles, often with dilation of the left atrium.<sup>32</sup>

Cardiomyocyte hypertrophy and disarray, a variable degree of interstitial fibrosis, interstitial inflammatory cell aggregates and dysplasia of vessel walls have been described most frequently as histological features of HCM.<sup>3,4,17,20</sup> In one study on familial HCM in domestic shorthair cats one end-stage case with multifocal areas of partly extensive myocardial fibrosis accompanied by a

mononuclear cell infiltration was reported; the changes were interpreted as myocardial infarcts.<sup>4</sup> Recent studies using a quantitative approach partially confirmed a diffuse or multifocal increase in interstitial fibrosis, but questioned cardiomyocyte hypertrophy and myofiber disarray as consistent features of HCM; they did neither find evidence of fiber branching nor significant differences in diameter and length of cardiomyocytes.<sup>3,16,17</sup> The inflammatory component in HCM has so far been characterized based on the cell morphology (hematoxylin-eosin stain) and limited cytochemical stains (Leder stain for neutrophils) and appears to comprise lymphocytes, plasma cells, neutrophils, and macrophages.<sup>4,17</sup> An ultrastructural study of the myocardium of cats with HCM identified degenerative changes, including mitochondrial damage, of cardiomyocytes and abundant extracellular matrix (ECM) deposition in the interstitium.<sup>6</sup>

The aim of the present study was to systematically assess the morphological changes and underlying mechanisms in feline HCM, to gain a better understanding of its complex pathophysiology. For this purpose, light microscopy was employed as a morphologic fact finding tool. This was followed by a quantitative, morphometric approach, which was complemented by a molecular investigation to assess the transcription of relevant markers and evaluate ongoing remodeling processes.

## **Materials and Methods**

### *Animals and Tissue Sampling*

The study was conducted on hearts of 36 cats (Table 1), 18 cats with HCM (Table 1A), and 18 control cats (i.e. cats that had died or were euthanized



with diseases not involving the heart; Table 1B). All HCM cats underwent a full post mortem examination with owners' consent. Two thirds (12/18) had been clinically confirmed and had undergone echocardiography carried out by a specialist in veterinary cardiology. The remaining six cases had been submitted for necropsy due to sudden death and clinical suspicion of cardiac disease. These cats showed marked left ventricular hypertrophy and left atrial dilation consistent with previously reported gross features of HCM,<sup>12</sup> in the absence of gross and histological changes suggestive of systemic disease. The majority of the control animals (12/18) had also undergone a full post mortem examination, the remaining third (6/18) were only available for a partial necropsy, and the diagnosis relied on the clinical examination and the gross assessment of the heart by the cardiologist. Samples for histology were collected from the right ventricular free wall (RV), left ventricular free wall (LV) and interventricular septum (IVS) and fixed in 10% neutral-buffered formalin. From 11 HCM and 10 control animals (of these, hearts had been removed within 1 h after death; Table 1), samples from each cardiac location were placed in RNAlater (Ambion, Life Technologies, Paisley, UK) and frozen at -80°C for subsequent RNA extraction.<sup>10</sup> From two animals (case nos. 1.8, 1.9; Table 1), additional myocardial samples were fixed in 5% glutaraldehyde, buffered in 0.2 M cacodylic acid buffer, pH 7.3, for transmission electron microscopy.

#### *Histology, Immunohistochemistry and Fluorescence Examinations*

After formalin fixation, myocardial samples were trimmed and routinely paraffin wax embedded. Consecutive sections (3 - 5 µm) were prepared and

routinely stained with hematoxylin-eosin (HE) and the van Gieson stain for the demonstration of collagen deposition, or were subjected to immunohistochemical and fluorescence staining. Immunohistochemistry was performed using a Dako autostainer (Dako, Glostrup, Denmark) or the Discovery XT autostainer (Ventana Medical System, Inc., Tucson, USA) and was applied to detect leukocytes (CD18+, MHC II+) and, specifically, T cells (CD3+), B cells (CD20+), macrophages (Iba-1+) and recently blood derived macrophages (calprotectin+), blood vessels, i.e. vascular endothelial cells (Factor VIII-related antigen (Factor VIII)+) and smooth muscle cells ( $\alpha$ -smooth muscle actin ( $\alpha$ -SMA)+). Antibodies and the respective antigen retrieval and detection methods are listed in Table 2. Briefly, after deparaffinization, antigen retrieval was performed for all antigens except for  $\alpha$ -SMA, by incubation of the slides with citrate buffer (pH 6) at 98°C for 10 min or EDTA buffer (pH 9) at 98°C for 20 min. Endogenous peroxidase was blocked by incubation with hydrogen peroxide solution for 10 min. Slides were incubated with equine serum for 30 min at room temperature followed by the primary antibodies and matching secondary antibodies; different detection kits were then applied (Table 2). Sections were washed with phosphate buffered saline between each incubation step (pH 8). Finally, sections were counterstained with hematoxylin for 40 s and mounted. A further section underwent fluorescence staining to mark cell nuclei, using the ProLong Diamond Antifade Mountant with DAPI (4', 6-diamidino-2-phenylindole; Invitrogen, Carlsbad, USA). Briefly, after deparaffinization and rehydration, sections were incubated with DAPI for 24 h at room temperature in the dark.

### *Transmission Electron Microscopy (TEM)*

After glutaraldehyde fixation for 24 h, the myocardial specimens were trimmed and routinely embedded in epoxy resin. Toluidine blue-stained semithin sections (1.5  $\mu\text{m}$ ) were prepared to select areas of interest for the preparation of ultrathin sections (75 nm) that were contrasted with lead citrate and uranyl acetate and viewed with a Philips CM10, operating with a Gatan Orius Sc1000 digital camera (Gatan Microscopical Suite, Digital Micrograph).

### *Morphometric Analyses*

A morphometric approach was taken to quantify the overall cellularity of the myocardium, the interstitial cellularity as well as the amount of interstitial collagen and the interstitial space in HCM in comparison to the myocardium of control cats.

Slides stained for Iba-1 and  $\alpha$ -SMA, with the van Gieson stain, and for DAPI fluorescence were scanned using a digital slide scanner (NanoZoomer-XR C12000; Hamamatsu, Hamamatsu City, Japan) and evaluated with the computer program VIS (Visiopharm Integrator System, Version 5.0.4. 1382; Visiopharm, Hoersholm, Denmark). For all quantitative approaches, 20 regions of interest (ROIs) with a size of 2.37 mm<sup>2</sup> (the area of a high power field with one ocular of 22 mm field of view) were randomly selected in the LV and RV and the IVS of all hearts. The van Gieson stain served to assess the proportion of space occupied by collagen, the proportion of interstitial empty space (i.e. cell- and fiber-free space) and the proportion of space occupied by cardiomyocytes (i.e. contractile tissue), each as % area. A threshold classification allowed recognition of fibrous tissue (bright pink),

cardiomyocytes (yellow) and interstitial empty space (empty) in each ROI, and the results were expressed as % of assessed tissue per ROI.

Sections stained for Iba-1 were used to quantify the amount of macrophages in the interstitium. A threshold classification allowed recognition of positive (intense brown staining of the entire cytoplasm) and negative cells in each ROI, and the results were expressed as absolute number of positive nuclei per ROI. In a post-processing step, very small nuclei (nuclear area < 5  $\mu\text{m}^2$ ) were excluded from counting in order to avoid that areas of increased background staining were falsely classified as nuclei. Nuclei that occurred in groups were often mistakenly classified as only one nucleus by the program and were therefore excluded from automated counting (nuclear area > 120  $\mu\text{m}^2$ ). Sections stained for  $\alpha$ -SMA were used to determine the amount of small- to medium-sized vessels (identified as  $\alpha$ -SMA positive vascular rings). Sections stained with DAPI fluorescence served to assess the amount of nuclei and thereby the overall cellularity of the myocardium. The intensity of the DAPI channel in NDP.view was set to be at 150% with a  $\gamma$ -value of 1.5 for all scans. A median unsharp filter ( $x = 55$ ,  $y = 55$ ) to remove background variation was added to the blue color channel (RGB-B) as a pre-processing step. With this method, the nuclei of all cell types were counted (cardiomyocytes, interstitial cells, vascular endothelial cells and smooth muscle cells).

#### *Quantitative Reverse Transcriptase PCR (qRT-PCR) for Relevant Remodeling Mediators*

For the amplification of the cytokines interleukin (IL)-1, IL-2, IL-4, IL-6, IL-8, IL-

18, tumor necrosis factor (TNF)- $\alpha$ , transforming growth factor (TGF)- $\beta$ , interferon (IFN)- $\gamma$ , the matrix metalloproteinases (MMP)-2, -3, -13 and the tissue inhibitors of matrix metalloproteinases (TIMP)-1, -2, -3 published primer pairs and protocols were applied.<sup>10</sup>

### *Statistical Analysis*

Data from morphometric measurements and qRT-PCRs were entered into spreadsheets and statistical analysis was performed using a commercially available software package (IBM SPSS Statistics 21, Portsmouth, UK). Basic descriptive statistics (mean, median, variance, standard deviation, interquartile range and confidence interval) were calculated for the variables recorded. Distribution of data was analysed applying graphical Q-Q plots, Kolmogorov Smirnov and Shapiro-Wilk analyses. Data from morphometric measurements and qRT-PCR results were not normally distributed and log transformed to improve normality and the model assumptions necessary for parametric analysis. Results between groups and regions were compared using 1-way ANOVA and Tukeys post hoc and unpaired t-tests. Scatter plots and linear regression analysis was used to investigate the relationship between data from morphometric measurements and age. Results are displayed as mean and standard deviation. Statistical significance was defined as  $p < 0.05$ .

## **Results**

### *Study population*

The group of 18 HCM cats (Table 1A) comprised one female, two male and

15 male neutered cats with a mean age of 7.6 years ( $\pm 3.06$  years) and a mean body weight of 5.6 kg ( $\pm 1.8$  kg). Three cats (1.7, 1.10, 1.11), all male neutered exhibited a left AT; with a mean age of 10 years ( $\pm 2.6$  years), they were older than the remaining 15 HCM cats without AT (mean age: 7.1 years ( $\pm 2.9$  years)).

The group of 18 control cats (Table 1B) comprised one female, 11 female neutered, two male and four male neutered cats. Their mean age of 7.7 years ( $\pm 4.8$  y) was similar to that of the HCM group. The mean body weight was 3.9 kg ( $\pm 1.1$  kg) and thereby significantly lower than the mean body weight of the HCM cats ( $p=0.001$ ).

Of the 11 HCM cats examined by qRT-PCR, 10 were male neutered and one was male intact. The cats had a mean age of 8.5 years ( $\pm 3.2$  y) and a mean body weight of 5.3 kg ( $\pm 1.8$  kg). The ten control cats examined by qRT-PCR were female neutered animals, except one male and one male neutered. Their mean age was 10 years ( $\pm 5.1$  years), which was similar to that of the HCM cats ( $p=0.215$ ).

*The composition of the feline myocardium is influenced by age.*

The unaltered myocardium (RV, LV, IVS) of the control cats was morphometrically assessed for a range of parameters (cellularity, amount of interstitial vessels ( $\alpha$ -SMA+) and macrophages (Iba-1+), proportion of area covered by cardiomyocytes (i.e. contractile tissue) and by the interstitium) to identify any regional and/or age-related variation (Table 3). This did not show regional differences (Table 3B), but a weak negative correlation of age with overall cellularity and proportion of contractile tissue, as well as a moderate

negative correlation of age with the amount of small vessels and macrophages in the interstitium (Table 3C). Interestingly, there was a weak negative correlation of age and the amount of interstitial collagen in HCM (Table 3C).

*HCM is associated with an increase in interstitial macrophages and small- to medium-sized vessels and a regional increase in interstitial collagen.*

All hearts were screened for histological features repeatedly described in HCM, i.e. cardiomyocyte disarray and degeneration, leukocyte infiltration and interstitial fibrosis.<sup>3,4,11,17,20</sup> Some or all of the above listed features were observed in most HCM cases (15/18; 83%). There was patchy to disseminated mild multifocal loss and/or degeneration of cardiomyocytes, the latter represented by loss of striation and occasional intracytoplasmic microvacuolization (Fig. 1), and variably intense, slight to mild multifocal interstitial collagen deposition (Figs. 2, 3) together with the presence of spindloid cells (fibroblasts; Fig. 2) that were occasionally  $\alpha$ -SMA positive (myofibroblasts).

In addition, all HCM cases exhibited evidence of mild diffuse interstitial widening (Fig. 1), occasional interstitial accumulations of mature adipocytes (fatty infiltration) and an increased interstitial cellularity (Figs. 2, 3). The latter was mainly due to the presence of mononuclear cells with macrophage morphology, i.e. round to spindle-shaped cells with a moderate to high amount of cytoplasm and an oval to round nucleus (Fig. 2). The majority of these cells exhibited strong Iba-1 (Fig. 4a) and MHC II expression (Fig. 4b) but were calprotectin-negative (Fig. 4c), suggesting that they were resident or

formerly blood-derived macrophages which had proliferated locally, rather than recently blood derived macrophages.<sup>34</sup> A few individual cells in the interstitium were identified as T cells (CD3+) and B cells (CD20+). Occasional small to medium-sized intramural vessels showed mild media hypertrophy, without significant narrowing of the lumen.

The quantitative assessment confirmed a significant increase in interstitial Iba-1- positive cells in HCM cats across all three assessed localisations, and an overall significant increase in interstitial small to medium sized vessels, which was due to a significant difference in IVS and LV. Alongside this, the amount of interstitial collagen was significantly higher in the IVS of HCM cats compared to controls. The results are detailed in Table 3A and B.

*In HCM, the myocardium frequently exhibits focal areas of cardiomyocyte replacement by cell rich fibrous tissue.*

In eight of the 18 HCM hearts (44%), the myocardium exhibited one or more poorly delineated areas where cardiomyocytes were replaced by a cell rich infiltrate (Fig. 5) with degenerate (shrinkage, loss of striation, hypereosinophilia, intracytoplasmic vacuolization) and rare necrotic cardiomyocytes in the periphery (Fig. 6). The core of these lesions was represented by densely-packed collagen bundles into which spindloid cells (fibroblasts) and mononuclear cells with a morphology similar to those found in increased numbers in the interstitium were embedded (Fig. 7). The latter cells were also Iba-1- (Fig. 8a) and MHC II-positive, but calprotectin-negative. Scattered T cells (CD3+) and B cells (CD20+) were also found. Between the Iba-1-positive cells were abundant small to medium-sized vessels, confirmed



by the ring-like structures formed and identified by Factor VIII-positive endothelial cells, as well as  $\alpha$ -SMA-positive pericytes and vascular wall associated smooth muscle cells (Fig. 8b). A few individual spindle-shaped cells were also found to express  $\alpha$ -SMA (myofibroblasts) (Fig. 8b). The degeneration of individual cardiomyocytes in the periphery of the focal lesions was confirmed by TEM (Fig. 9). Individual or multiple cardiomyocytes were found embedded and walled off by dense and partially irregularly arranged collagen fiber bundles (Fig. 9b, 9c), and showed myofiber disarray and disruption of intercalated discs with marked disorganization and interdigitation of Z-lines (Fig. 9d).

*The pathological changes in the myocardium with HCM are associated with significant upregulation of pro-inflammatory and pro-fibrotic mediators.*

Quantitative RT-PCR results confirmed the constitutive expression of cytokines, MMPs and TIMPs in the myocardium of all cats.<sup>10</sup> However, cats with HCM showed significantly higher transcription levels for IL-1, IL-6, IL-18, TNF- $\alpha$ , TGF- $\beta$ , MMP-13, and TIMP-1 (Table 4A). As previously reported, control cats exhibited a moderate positive correlation of age and myocardial TGF- $\beta$  transcription and a moderate negative correlation of IL-4 mRNA levels and age.<sup>10</sup> For HCM cats a strong negative correlation with age was observed for IL-8, MMP-2 and MMP-13, a moderate negative correlation for IFN- $\gamma$ , TGF- $\beta$ , MMP-3 and TIMP-2, and a weak negative correlation for IL-2 and IL-4 (Table 4B).

## Discussion

Feline HCM is a disease with a complex pathophysiology that is yet far from clear. Several studies have been carried out in recent years to characterize and quantify its morphological features, reporting fibrosis, myofiber disarray or hypertrophy, and inflammatory components.<sup>3,4,16,17,20</sup> Their results are, at least in part, controversial which left open many questions on the pathogenesis of this relevant entity.<sup>29</sup>

We have recently shown that the normal myocardium of cats is actively transcribing a range of inflammatory and remodeling mediators, with a clear age- and sex-related variation and a shift from a pro-inflammatory state in young age to a pro-fibrotic state with increasing age; the former being more pronounced in male cats.<sup>10</sup> Considering also that HCM is a disease particularly of older, intact or neutered male cats,<sup>1,25,29</sup> we aimed to further investigate the pathological features of the myocardium in HCM, with particular emphasis on the associated remodeling processes.

Grossly, all HCM hearts exhibited the typical diffuse thickening of the LV and/or the IVS and a dilation of the left atrium.<sup>12</sup> Histology confirmed the presence of several previously described features, i.e. cardiomyocyte disarray and degeneration and interstitial fibrosis, as well as leukocyte infiltration, in most cases.<sup>2-4,17,20</sup> Other studies described marked media hypertrophy, fibrosis and elastosis of intramural vessels in feline HCM.<sup>12,20</sup> These features were not prominent in our HCM cohort where the vascular changes were restricted to mild media hypertrophy in small to medium-sized intramural vessels. However, the present study identified several additional, rather subtle, but consistent and statistically significant quantitative changes: an

overall increase in the amount of interstitial Iba-1-positive mononuclear cells, small and medium sized vessels, and collagen. The difference was most reliably demonstrated in the IVS, followed by the LV, whereas in the RV, the quantitative changes were restricted to the increased amount of interstitial Iba-1-positive cells. Interestingly, the increase in interstitial cells was not associated with an increase in overall cell numbers, suggesting a reduction of cardiomyocytes, which is indirect evidence of some degree of diffuse cardiomyocyte injury and loss. Immunohistochemistry confirmed the mononuclear interstitial cells as macrophages, as these were in the vast majority not only Iba-1-, but also MHC II-positive. The lack of calprotectin expression suggests that they were resident or locally proliferated macrophages, rather than recently recruited from the blood into the myocardium.<sup>34</sup> T cells and B cells were not more numerous in HCM than in the control myocardium.

The focal lesions, which were found in addition to the diffuse changes in a large proportion of HCM hearts, were most prominent in IVS and LV, i.e. the regions that show the characteristic thickening and were found to exhibit the most severe diffuse changes. These focal infiltrates, with their core of fibrous tissue and abundant embedded macrophages and new vessels, are reminiscent of infarct-like lesions and disorderly arranged granulation tissue.<sup>4,7,13</sup> The presence of dying cardiomyocytes in the periphery, where they seem to be walled off by collagen fibers, suggests that these infiltrates are actively expanding. Their random distribution indicates that they are initiated by focal tissue damage, i.e. cardiomyocyte death.

The findings suggest that HCM is not of a classical inflammatory nature with

persistent recruitment and interaction of inflammatory cells in the myocardium. Instead, also in light of the significant increase in interstitial small vessels and the diffuse interstitial collagen deposition, a diffuse macrophage-driven remodeling process is suspected. The interstitial macrophages could represent a primary inflammatory component, and their recruitment and proliferation could be initiated by the myocardium itself. Cardiomyocytes are a known source of cytokines, constitutively transcribing a panel of inflammatory and profibrotic mediators, e.g. IL-1, IL-6, TNF- $\alpha$ , INF- $\gamma$  and TGF- $\beta$ .<sup>10</sup> Their expression can be enhanced by cardiomyocyte injury.<sup>27</sup> Activated macrophages could then be responsible for the formation of new interstitial vessels, the proliferation respectively activation of fibroblasts and the occurrence of myofibroblasts as well as the deposition of interstitial collagen, through the release of angiogenic and fibrogenic mediators. Indeed, we found a significant increase in the transcription of inflammatory (IL-1, IL-6, IL-18, TNF- $\alpha$ ) and profibrotic (TGF- $\beta$ , MMP-13, and TIMP-1) mediators in HCM. Involvement of inflammatory cytokines in myocardial remodeling in feline HCM is therefore likely, and both the cardiomyocytes and abundant macrophages might be the sources.<sup>10,14,33</sup>

Together, new vessel formation, fibroblast proliferation and collagen deposition in the focal lesions represent key events in granulation tissue formation.<sup>19</sup> Angiogenesis in general represents a fundamental component of repair processes and is critical for the maintenance of the required blood flow at sites of injury or ischemia.<sup>46</sup> Fibroblasts then migrate into the damaged tissue and produce collagen-rich connective tissue to maintain the structural integrity.<sup>19,36</sup>

In HCM, the diffuse increase in interstitial vessels is likely also due to new vessel formation, which is known to be triggered by hypoxia.<sup>18</sup> Low oxygen levels lead to up-regulation of various pro-angiogenic pathways promoting increased vessel sprouting.<sup>18</sup> In humans it has been shown that compared to their normoxic counterparts, cardiomyocytes exposed to constant hypoxia have elevated secretion levels of inflammatory cytokines, including IL-1, IL-6, IL-8, as well as certain growth factors and chemokines.<sup>15</sup>

The initial cause of myocardial damage in feline HCM that would trigger the observed remodeling processes is still unknown, but hypoxia appears likely considering the present findings.<sup>4,12</sup> So far unknown structural or functional myocardial alterations could result in latent myocardial hypoxia, leading to individual cardiomyocyte degeneration and death. Focally pronounced or chronic hypoxia could then result in a larger area of cardiomyocyte necrosis, leading to the observed focal lesions. Here, the release of chemokines and cytokines and dead cardiomyocytes can induce recruitment and proliferation of macrophages which subsequently clear the cellular debris and secrete those chemokines and cytokines that are responsible for all other processes.<sup>5,30</sup> This hypothesis is supported by the observed increase in vessels in our case cohort and by the fact that a hypoxic environment can induce a macrophage driven inflammatory response, where recruited, blood-derived monocytes differentiate into macrophages that reside in areas of hypoxic damage.<sup>26</sup>

In human HCM patients, myocardial ischemia is the result of changes in the coronary arteriolar microvasculature.<sup>21,22,35</sup> In our feline cohort, there is no evidence of a similar scenario in cats.<sup>12</sup>

We have previously shown that the myocardium of young, male cats is in a pronounced pro-inflammatory and potentially alerted state.<sup>10</sup> This might provide a favourable environment for cardiomyocyte damage, if appropriately triggered. Alternatively, susceptible cats might exhibit persistent endogenous upregulation of cytokines, which would render cardiomyocytes more prone to injury even after mild hypoxic events.

Also, with age the hearts of humans undergo various functional and morphological changes, including a thickening of the LV, gradual decline of the number of cardiomyocytes accompanied by an increase of collagen, fibrotic changes in the valves, and vascular remodeling with progressive intimal thickening.<sup>9</sup> We have not observed similarly striking processes in the myocardium of old cats without cardiac disease, but have previously shown that the myocardial mediator transcription pattern shifts from a pro-inflammatory state in young animals to a pro-fibrotic state in age.<sup>10</sup> The morphometric analysis of the present study now adds data on age-related changes in the composition of the myocardium: with age, the cellularity, the amount of interstitial blood vessels and macrophages, and the proportion of contractile tissue decreases, suggesting a decreased reactivity and with it, possibly, repair of the myocardium of older cats. Such impaired cardiac repair, alongside continuous, slow disease progression could lead to the observed and more pronounced damage with reduced tissue and immune reaction in older animals. This might also promote AT formation, as the cats with AT in our HCM cohort were older than those without AT.

In conclusion, the results of our study provide further evidence that the increase in wall thickness and relative cardiac weight in feline HCM is not the

result of true myocardial hypertrophy, but due to a diffuse expansion of the interstitium by vessels, macrophages and collagen as a consequence of degeneration and repair processes triggered by a still unknown cause. In HCM, the hearts seem to exhibit a long-term, progressive myocardial remodeling process. On a cellular level this process is likely driven by cardiomyocytes and local macrophages. Further studies are required to identify the type and source of these macrophages and further specify their role in the pathogenetic process of feline HCM.

### **Acknowledgements**

We thank the technical staff of the Histology Laboratory and the TEM Unit, Institute of Veterinary Pathology, Vetsuisse Faculty, University of Zurich, as well as the staff of the Histology Laboratory, Faculty of Veterinary Medicine, University of Helsinki, for excellent technical assistance.

## References

1. Abbott JA. Feline hypertrophic cardiomyopathy: An update. *Vet Clin North Am - Small Anim Pract.* 2010;40(4):685–700.
2. Aupperle H, Baldauf K, März I. An immunohistochemical study of feline myocardial fibrosis. *J Comp Pathol.* 2011;145(2-3):158–173.
3. Biasato I, Francescone L, La Rosa G, Tursi M. Anatomopathological staging of feline hypertrophic cardiomyopathy through quantitative evaluation based on morphometric and histopathological data. *Res Vet Sci.* 2015;102:136–141.
4. Cesta MF, Baty CJ, Keene BW, Smoak IW, Malarkey DE. Pathology of end-stage remodeling in a family of cats with hypertrophic cardiomyopathy. *Vet Pathol.* 2005;42(4):458–467.
5. Chen B, Frangogiannis NG. Macrophages in the remodeling failing heart. *Circ Res.* 2016;119(7):776–778.
6. Christiansen LB, Prats C, Hyttel P, Koch J. Ultrastructural myocardial changes in seven cats with spontaneous hypertrophic cardiomyopathy. *J Vet Cardiol.* 2015;17:220–232.
7. Dobaczewski M, Gonzalez-Quesada C, Frangogiannis NG. The extracellular matrix as a modulator of the inflammatory and reparative response following myocardial infarction. *J Mol Cell Cardiol.* 2010;48(3):504–511.
8. Ferasin L, Sturgess CP, Cannon MJ, Caney SMA, Gruffydd-Jones TJ, Wotton PR. Feline idiopathic cardiomyopathy: a retrospective study of 106 cats (1994-2001). *J Feline Med Surg.* 2003;5(3):151–159.



9. Fleg JL, Strait J. Age-associated changes in cardiovascular structure and function: a fertile milieu for future disease. *Heart Fail Rev.* 2012;17:545–554.
10. Fonfara S, Hetzel U, Hahn S, Kipar A. Age- and gender-dependent myocardial transcription patterns of cytokines and extracellular matrix remodelling enzymes in cats with non-cardiac diseases. *Exp Gerontol.* 2015;72:117–123.
11. Fox PR, Maron BJ, Basso C, Liu SK, Thiene G. Spontaneously occurring arrhythmogenic right ventricular cardiomyopathy in the domestic cat: A new animal model similar to the human disease. *Circulation.* 2000;102:1863–1870.
12. Fox PR. Hypertrophic cardiomyopathy. Clinical and pathologic correlates. *J Vet Cardiol.* 2003;5(2):39–45.
13. Frangogiannis NG. Regulation of the inflammatory response in cardiac repair. *Circ Res.* 2012;110(1):159–173.
14. Frangogiannis NG. The inflammatory response in myocardial injury, repair, and remodelling. *Nat Rev Cardiol.* 2014;11:255-262.
15. Hafner C, Wu J, Tiboldi A, et al. Hyperoxia induces inflammation and cytotoxicity in human adult cardiac myocytes. *Shock.* 2017;47(4):436–444.
16. Kershaw O, Heblinski N, Lotz F, Dirsch O, Gruber AD. Diagnostic value of morphometry in feline hypertrophic cardiomyopathy. *J Comp Pathol.* 2012;147(1):73–83.
17. Khor KH, Campbell FE, Owen H, Shiels IA, Mills PC. Myocardial

- collagen deposition and inflammatory cell infiltration in cats with pre-clinical hypertrophic cardiomyopathy. *Vet J*. 2015;203(2):161–168.
18. Krock BL, Skuli N, Simon MC. Hypoxia-induced angiogenesis: good and evil. *Genes Cancer*. 2011;2(12):1117–1133.
  19. Kumar V, Stanley L, Cotran RS. Inflammation and repair: tissue repair. In: Kumar V, Abbas AK, Aster JC, Robbins SL, ed. *Robbins and Cotran Pathologic Basis of Disease*. Philadelphia: Elsevier; 2015:100–111.
  20. Liu SK, Maron BJ, Tilley LP. Feline hypertrophic cardiomyopathy: gross anatomic and quantitative histologic features. *Am J Pathol*. 1981;102(3):388–395.
  21. Maron BJ, Wolfson JK, Epstein SE, Roberts WC. Intramural (“small vessel”) coronary artery disease in hypertrophic cardiomyopathy. *J Am Coll Cardiol*. 1986;8(3):545–557.
  22. Maron BJ. Hypertrophic cardiomyopathy. *JAMA*. 2002 Mar 13;287(10):1308–1320.
  23. Meurs KM, Norgard MM, Ederer MM, Hendrix KP, Kittleson MD. A substitution mutation in the myosin binding protein C gene in ragdoll hypertrophic cardiomyopathy. *Genomics*. 2007;90:261–264.
  24. Meurs KM, Sanchez X, David RM, et al. A cardiac myosin binding protein C mutation in the Maine Coon cat with familial hypertrophic cardiomyopathy. *Hum Mol Genet*. 2005;14(2):3587–3593.
  25. Migliorini F. Miocardiopatie feline. *Man di Cardiol del Cane e del Gatto, Prima Ed*. 2012;205–224.
  26. Murdoch C, Giannoudis A, Lewis CE. Mechanisms regulating the

- recruitment of macrophages into hypoxic areas of tumors and other ischemic tissues. *Blood*. 2004;104(8):2224-2234.
27. Noji Y, Shimizu M, Ino H, et al. Increased circulating matrix metalloproteinase-2 in patients with hypertrophic cardiomyopathy with systolic dysfunction. *Circ J*. 2004;68(4):355–360.
  28. Payne JR, Borgeat K, Brodbelt DC, Connolly DJ, Luis Fuentes V. Risk factors associated with sudden death vs. congestive heart failure or arterial thromboembolism in cats with hypertrophic cardiomyopathy. *J Vet Cardiol*. 2015;17:318–328.
  29. Payne JR, Brodbelt DC, Luis Fuentes V. Cardiomyopathy prevalence in 780 apparently healthy cats in rehoming centres (the CatScan study). *J Vet Cardiol*. 2015;17:244–257.
  30. Raggi F, Blengio F, Eva A, Pende D, Varesio L, Bosco MC. Identification of CD300a as a new hypoxia-inducible gene and a regulator of CCL20 and VEGF production by human monocytes and macrophages. *Innate Immun*. 2013;20(7):721–734.
  31. Riesen SC, Kovacevic A, Lombard CW, Amberger C. Prevalence of heart disease in symptomatic cats: An overview from 1998 to 2005. *Schweiz Arch Tierheilkd*. 2007;149(2):65–71.
  32. Robinson WN, Robinson NA. Myocardial disease: cardiomyopathies. In: Maxie MG, ed. *Jubb, Kennedy & Palmer's Pathology of Domestic Animals*. St.Louis, Missouri; 2016:44–50.
  33. Soehnlein O, Lindbom L. Phagocyte partnership during the onset and resolution of inflammation. *Nat Rev Immunol*. 2010;10:427.

34. Susta L, Torres-Velez F, Zhang J, Brown C. An in situ hybridization and immunohistochemical study of cytauxzoonosis in domestic cats. *Vet Pathol.* 2009;46(6):1197–1204.
35. Waller BF, Maron BJ, Epstein SE, Roberts WC. Transmural myocardial infarction in hypertrophic cardiomyopathy. *Chest.* 2018;79(4):461–465.
36. Weber KT, Anversa P, Armstrong PW, et al. Remodeling and reparation of the cardiovascular system. *J Am Coll Cardiol.* 1992;20(1):3–16.

**Table 1.** Animals included into the study. In all cases, a histological and immunohistological examination including a morphometric analysis were undertaken.

**A.** Cats diagnosed with hypertrophic cardiomyopathy (HCM).

<b>Case No</b>	<b>Breed</b>	<b>Age (years)</b>	<b>Sex</b>
1.1 <sup>a</sup>	DSH	10	M
1.2 <sup>a</sup>	DLH	8	MN
1.3 <sup>a</sup>	DSH	3	MN
1.4 <sup>a</sup>	DSH	8	MN
1.5 <sup>a</sup>	DSH	7	MN
1.6 <sup>a</sup>	BSH	8	MN
1.7 <sup>a</sup>	DLH	12	MN
1.8 <sup>a,b</sup>	Ragdoll	3	MN
1.9 <sup>a,b</sup>	DSH	9	MN
1.10 <sup>a</sup>	DSH	14	MN
1.11 <sup>a</sup>	DLH	8	MN
1.12	MC	6	MN
1.13	DSH	3	M
1.14	MC	4	MN
1.15	Devon Rex	7	MN
1.16	DSH	11	MN
1.17	MC	1.5	F
1.18	DSH	6	MN

**B. Control animals.**

<b>Case No</b>	<b>Breed</b>	<b>Age (years)</b>	<b>Sex</b>
2.1 <sup>a</sup>	DSH	14	FN
2.2 <sup>a</sup>	DSH	18	FN
2.3 <sup>a</sup>	DSH	14	M
2.4 <sup>a</sup>	DSH	10	FN
2.5 <sup>a</sup>	DSH	2	FN
2.6 <sup>a</sup>	DSH	15	FN
2.7 <sup>a</sup>	DSH	3	FN
2.8 <sup>a</sup>	DSH	9	FN
2.9 <sup>a</sup>	DSH	10	FN
2.10 <sup>a</sup>	DSH	5	MN
2.11	DSH	6	MN
2.12	DSH	5	MN
2.13	DLH	5	FN
2.14	DSH	2.5	FN
2.15	DSH	4	M
2.16	DSH	4	F
2.17	DSH	2.5	FN
2.18	DSH	9	MN

BSH, British Shorthair; DLH, Domestic Longhair; DSH, Domestic Shorthair; F, female; HCM, hypertrophic cardiomyopathy; M, male; MC, Maine Coon; N, neutered.

a: qRT-PCR undertaken; b: TEM undertaken

**Table 2.** Antibodies and immunohistological methods.

Antigen	Expression	Antibody (clone)	Source	Dilution
CD3	T cells	Mouse mAb (F.7.2.38)	Dako	1:200
CD20	B cells	Rabbit pAb	Thermo Scientific	1:1000
Factor VIII (-related Ag)	Endothelial cells, megakaryo- cytes, platelets, mast cells	Rabbit pAb	Dako	1:100
MHC II (HLA-DR)	Macrophages, B and T cells, dendritic cells	Mouse mAb (TAL 1B5)	Abcam	1:1500
Iba-1	Microglia, macrophages	Rabbit pAb	Wako	1:750
$\alpha$ -SMA	Smooth muscle cells, myo- fibroblasts, myoepithelial cells	Mouse mAb (1A4)	Dako	1:400

Ag, antigen;  $\alpha$ -SMA,  $\alpha$ -smooth muscle actin; CD, cluster of differentiation; Citrate, citrate buffer pretreatment; EDTA, EDTA pretreatment; HLA-DR, human leukocyte antigen – antigen D related; HRP, horseradish peroxidase; Iba-1, ionized calcium binding adaptor molecule 1; mAb, monoclonal antibody; MHC, major histocompatibility complex; n/d, not done; pAb, polyclonal antibody.



**Table 3.** Comparison of overall cellularity, number of interstitial small vessels and macrophages (i.e. Iba-1+ cells), and percentage of area covered by cardiomyocytes, collagen and fiber- and cell-free interstitial space as well as the ratio of contractile and non-contractile tissue in the myocardium (right and left ventricle, interventricular septum) of 18 control cats and 18 cats with HCM.

**A.** Overall assessment, based on the available data for all three cardiac regions (mean  $\pm$  standard deviation).

	<b>Control</b>	<b>HCM</b>	<b>P-value</b>
DAPI	3.1 ( $\pm$ 0.8)	3.0 ( $\pm$ 0.9)	0.066
SMA	2.2 ( $\pm$ 0.4)	2.4 ( $\pm$ 0.3)	<b>0.001</b>
Iba-1	0.9 ( $\pm$ 0.4)	1.6 ( $\pm$ 0.4)	<b>&lt;0.001</b>
Cardiomyocytes	1.9 ( $\pm$ 0.05)	1.9 ( $\pm$ 0.1)	0.18
Collagen	0.62 ( $\pm$ 0.3)	0.74 ( $\pm$ 0.2)	<b>0.039</b>
Interstitial space	1.25 ( $\pm$ 0.2)	1.3 ( $\pm$ 0.3)	0.23
Contractile vs non-contractile tissue ratio	0.78 ( $\pm$ 0.3)	0.71 ( $\pm$ 0.3)	0.27

DAPI: number of cells per 20 ROI, based on the number of DAPI positive fluorescent nuclei; SMA: number of  $\alpha$ -SMA positive small to medium sized vessels per 20 ROI; Iba-1: number of Iba-1 positive interstitial cells per 20 ROI; cardiomyocytes: percentage area per 20 ROI covered by cardiomyocytes (i.e. contractile tissue); collagen: percentage area per 20 ROI covered by collagen; interstitial space: percentage area per 20 ROI of fiber- and cell-free interstitial space

DAPI, 4', 6-diamidino-2-phenylindole; Iba-1, ionized calcium-binding adapter molecule 1; SMA,  $\alpha$ -smooth muscle actin.

**B. Comparison of the different cardiac regions (median, interquartile range).**

When the numbers of samples analysed differed from sample numbers provided for each region, the analysed numbers of samples are provided accordingly in the table. Results that are significantly different within rows are indicated by superscript symbols.

	<b>Control</b>			<b>HCM</b>		
	RV	IVS	LV	RV	IVS	LV
	(n=18)	(n=18)	(n=18)	(n=12)	(n=14)	(n=13)
DAPI	3.0 ( $\pm$ 0.1)	3.1 ( $\pm$ 0.1)	3.1 ( $\pm$ 0.1)	3.0 ( $\pm$ 0.1)	3.0 ( $\pm$ 0.1)	3.0 ( $\pm$ 0.1)
	n=14	n=14	n=14		n=12	n=14
SMA	2.2 ( $\pm$ 0.4)	2.2 ( $\pm$ 0.4) <sup>@</sup>	2.2 ( $\pm$ 0.5) <sup>\$</sup>	2.3 ( $\pm$ 0.3)	2.5 ( $\pm$ 0.2) <sup>@</sup>	2.5 ( $\pm$ 0.3) <sup>\$</sup>
				n=14	n=15	n=17
Iba-1	0.9 ( $\pm$ 0.5) <sup>*</sup>	1.0 ( $\pm$ 0.4) <sup>&amp;</sup>	1.0 ( $\pm$ 0.4) <sup>^</sup>	1.4 ( $\pm$ 0.4) <sup>*</sup>	1.6 ( $\pm$ 0.5) <sup>&amp;</sup>	1.7 ( $\pm$ 0.4) <sup>^</sup>
				n=15	n=16	n=16
Cardiomyocytes	1.9 ( $\pm$ 0.06)	1.9 ( $\pm$ 0.05)	1.9 ( $\pm$ 0.05)	1.9 ( $\pm$ 0.1)	1.9 ( $\pm$ 0.1)	1.9 ( $\pm$ 0.1)
Interstitial space	1.2 ( $\pm$ 0.3)	1.1 ( $\pm$ 0.3)	1.1 ( $\pm$ 0.3)	1.25 ( $\pm$ 0.3)	1.2 ( $\pm$ 0.3)	1.1 ( $\pm$ 0.4)
Collagen	0.7 ( $\pm$ 0.3)	0.5 ( $\pm$ 0.3) <sup>#</sup>	0.6 ( $\pm$ 0.3)	0.6 ( $\pm$ 0.2)	0.8 ( $\pm$ 0.2) <sup>#</sup>	0.8 ( $\pm$ 0.2)

Contractile vs non-

contractile tissue

0.7 ( $\pm$  0.3)

0.9 ( $\pm$  0.3)

0.8 ( $\pm$  0.2)

0.7 ( $\pm$  0.3)

0.7 ( $\pm$  0.3)

0.7 ( $\pm$  0.3)

ratio

---

**C.** Correlation of the different parameters with age in age-matched control cats (n=18) and cats with HCM (n=18), based on the available data for all three cardiac regions.

		<b>Control</b>	<b>HCM</b>
DAPI	R-value	0.368	0.276
	Significance	<b>0.017</b> ↓	0.094
SMA	R-value	0.455	0.228
	Significance	<b>0.001</b> ↓	0.128
Iba-1	R-value	0.511	0.065
	Significance	<b>&lt;0.001</b> ↓	0.666
Cardiomyocytes	R-value	0.278	0.095
	Significance	<b>0.042</b> ↓	0.565
Collagen	R-value	0.007	0.354
	Significance	0.962	<b>0.027</b> ↓
Interstitial space	R-value	0.241	0.108
	Significance	0.08	0.513
Contractile vs non- contractile tissue ratio	R-value	0.215	0.212
	Significance	0.118	0.196

↓ - indicates negative correlation, i.e. a decrease with age; ↑ - indicates positive correlation, i.e. an **Figure**

**legends**

**Table 4.** Cytokine and remodeling marker transcription in the myocardium of cats with and without hypertrophic cardiomyopathy.

**A.** Relative mRNA expression of cytokines and remodeling markers in the myocardium (interventricular septum, left and right ventricle) of control cats (n=10) and cats with HCM (n=11).

Marker	Control	HCM	P-value
IL-1	-0.036 ( $\pm 0.63$ )	0.34 ( $\pm 0.31$ ) $\uparrow$	<b>0.01</b>
IL-2	1.72 ( $\pm 0.46$ )	1.52 ( $\pm 0.62$ )	0.181
IL-4	1.38 ( $\pm 0.49$ )	1.29 ( $\pm 0.64$ )	0.592
IL-6	0.056 ( $\pm 0.56$ )	0.74 ( $\pm 1.1$ ) $\uparrow$	<b>0.01</b>
IL-8	1.88 ( $\pm 0.48$ )	1.39 ( $\pm 0.80$ )	0.083
IL-18	1.93 ( $\pm 0.67$ )	2.75 ( $\pm 0.75$ ) $\uparrow$	<b>&lt;0.001</b>
TNF- $\alpha$	-0.63 ( $\pm 0.73$ )	0.26 ( $\pm 0.45$ ) $\uparrow$	<b>&lt;0.001</b>
IFN- $\gamma$	2.11 ( $\pm 0.34$ )	2.0 ( $\pm 0.34$ )	0.455
TGF- $\beta$	2.20 ( $\pm 0.43$ )	2.52 ( $\pm 0.64$ ) $\uparrow$	<b>0.031</b>
MMP-2	2.64 ( $\pm 0.62$ )	2.75 ( $\pm 0.65$ )	0.536
MMP-3	1.53 ( $\pm 0.38$ )	1.46 ( $\pm 0.78$ )	0.669
MMP-13	0.48 ( $\pm 0.42$ )	0.93 ( $\pm 0.48$ ) $\uparrow$	<b>&lt;0.001</b>
TIMP-1	-0.41 ( $\pm 0.50$ )	-0.079( $\pm 0.51$ ) $\uparrow$	<b>0.039</b>
TIMP-2	4.01 ( $\pm 0.25$ )	3.88 ( $\pm 0.56$ )	0.244
TIMP-3	3.51 ( $\pm 0.51$ )	3.63 ( $\pm 0.95$ )	0.526

Results are reported as mean and standard deviation of the logarithmic value ( $2^{-\Delta\Delta Ct}$ ) after normalization of the Ct value of the respective marker to the Ct value of GAPDH (relative expression). P-values

indicating significant differences are in bold.

**B.** Correlation of cytokine and remodeling marker mRNA expression with age in control cats and cats with HCM, based on the available data for all three cardiac regions.

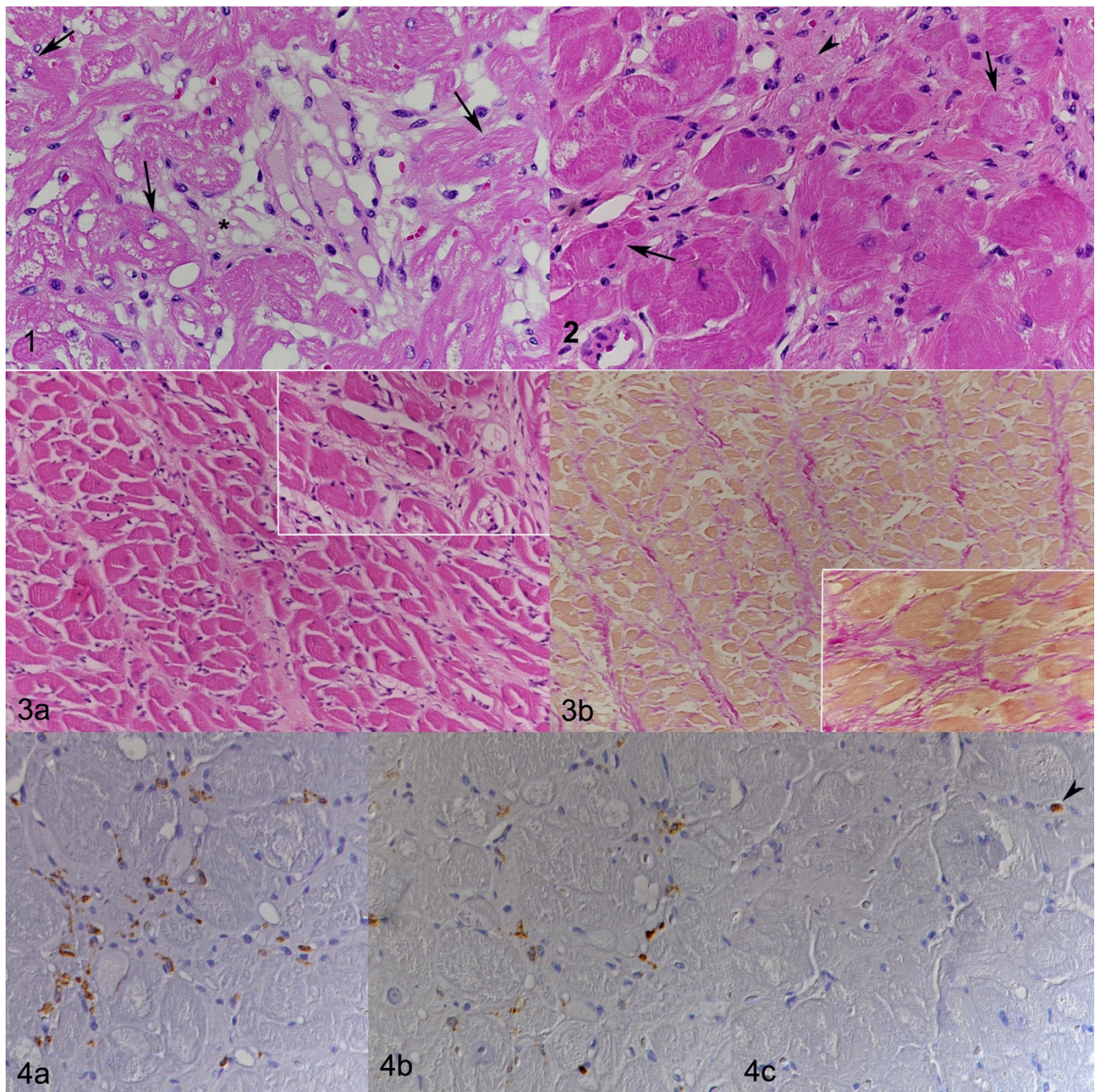
		<b>Control</b>	<b>HCM</b>
IL-1	R-value	0.357	0.193
	Significance	0.068	0.389
IL-2	R-value	0.207	0.357
	Significance	0.300	<b>0.049</b> ↓
IL-4	R-value	0.393	0.321
	Significance	<b>0.043</b> ↓	<b>0.019</b> ↓
IL-6	R-value	0.146	0.238
	Significance	0.478	0.263
IL-8	R-value	0.041	0.617
	Significance	0.910	<b>0.001</b> ↓
IL-18	R-value	0.075	0.197
	Significance	0.709	0.287
TNF- $\alpha$	R-value	0.238	0.224
	Significance	0.233	0.316
IFN- $\gamma$	R-value	0.187	0.435
	Significance	0.404	<b>0.014</b> ↓
TGF- $\beta$	R-value	0.432	0.526
	Significance	<b>0.028</b> ↑	<b>0.002</b> ↓
MMP-2	R-value	0.285	0.740
	Significance	0.150	<b>&lt;0.001</b> ↓
MMP-3	R-value	0.159	0.357

MMP-13	Significance	0.429	<b>0.049</b> ↓
	R-value	0.126	0.689
TIMP-1	Significance	0.531	<b>&lt;0.001</b> ↓
	R-value	0.103	0.017
TIMP-2	Significance	0.667	0.942
	R-value	0.068	0.590
TIMP-3	Significance	0.756	<b>&lt;0.001</b> ↓
	R-value	0.160	0.278
	Significance	0.425	0.129

---

↓ - indicates negative correlation, i.e. a decrease with age; ↑ - indicates positive correlation, i.e. an increase with age.

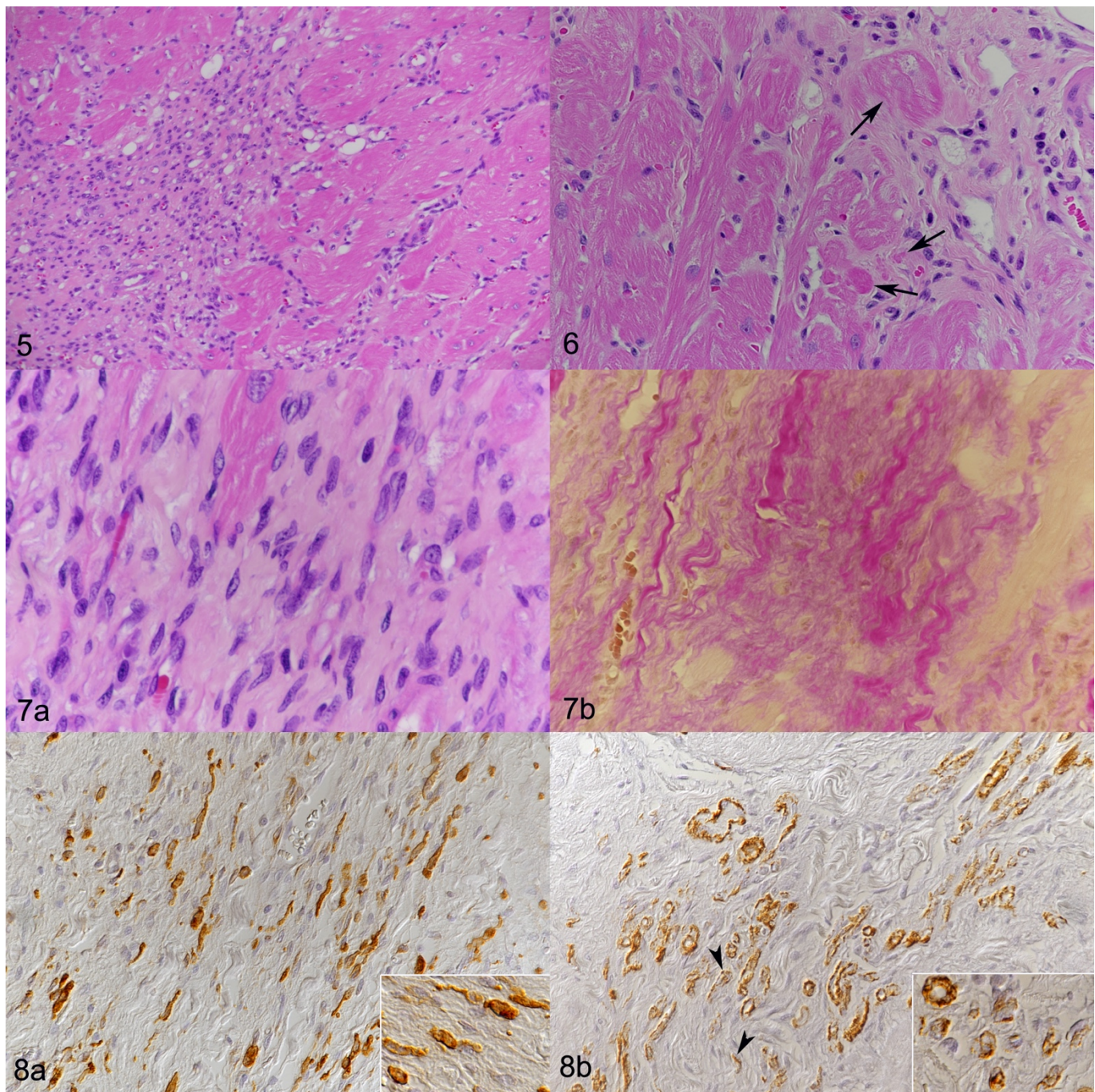
HCM, hypertrophic cardiomyopathy; IL, interleukin; IFN- $\gamma$ , interferon- $\gamma$ ; MMP, matrix metalloproteinase; TGF- $\beta$ , transforming growth factor- $\beta$ ; TIMP, tissue inhibitor of metalloproteinases; TNF- $\alpha$ , tumor necrosis factor- $\alpha$ .



**Figures 1-4.** Hypertrophic cardiomyopathy (HCM), heart, cat, case no 1.8. Diffuse myocardial changes. **Figure 1.** There are individual degenerating cardiomyocytes that exhibit loss of striation and cytoplasmic microvacuolization (arrows); the interstitium appears widened (asterisk). HE stain. **Figure 2.** Mild interstitial collagen deposition (arrowhead) with presence of several fibroblasts and other mononuclear cells. Arrows: degenerating cardiomyocytes with loss of



striation. HE stain. **Figure 3.** Overview to highlight the widespread nature of interstitial collagen deposition and the increased interstitial cellularity. Insets: higher magnification. (a) HE stain, (b) van Gieson stain. **Figure 4.** A high proportion of the interstitial mononuclear cells exhibit Iba-1 (a) and MHC II (b) expression, but are calprotectin-negative (c). Arrowhead: calprotectin-positive monocyte within interstitial vessel. Immunohistochemistry, hematoxylin counterstain.



**Figures 5-8.** Hypertrophic cardiomyopathy (HCM), heart, cat, case no 1.9. Focal lesions. **Figure 5.** Cardiomyocytes are replaced by a poorly delineated cell rich infiltrate. HE stain. **Figure 6.** Periphery of a focal lesion, with individual cardiomyocytes (arrows) that exhibit degenerative changes, such as shrinkage, loss of striation and hypereosinophilia. HE stain. **Figure 7.** The core of these lesions is comprised of densely-packed collagen bundles into which spindloid cells

(fibroblasts) and mononuclear cells with a macrophage morphology are embedded. Small vessels are also seen. (a) HE stain, (b) van Gieson stain. **Figure 8.** (a) A large proportion of the cells in the lesion are Iba-1-positive (inset: higher magnification to illustrate the morphology of the Iba-1-positive cells). (b) In addition, there are numerous small to medium-sized vessels, confirmed by ring-like structures of  $\alpha$ -SMA-positive pericytes and smooth muscle cells that comprise the media (inset). There are also individual  $\alpha$ -SMA-positive spindloid, fibroblast-like cells consistent with myofibroblasts (arrowheads). Immunohistochemistry, hematoxylin counterstain.



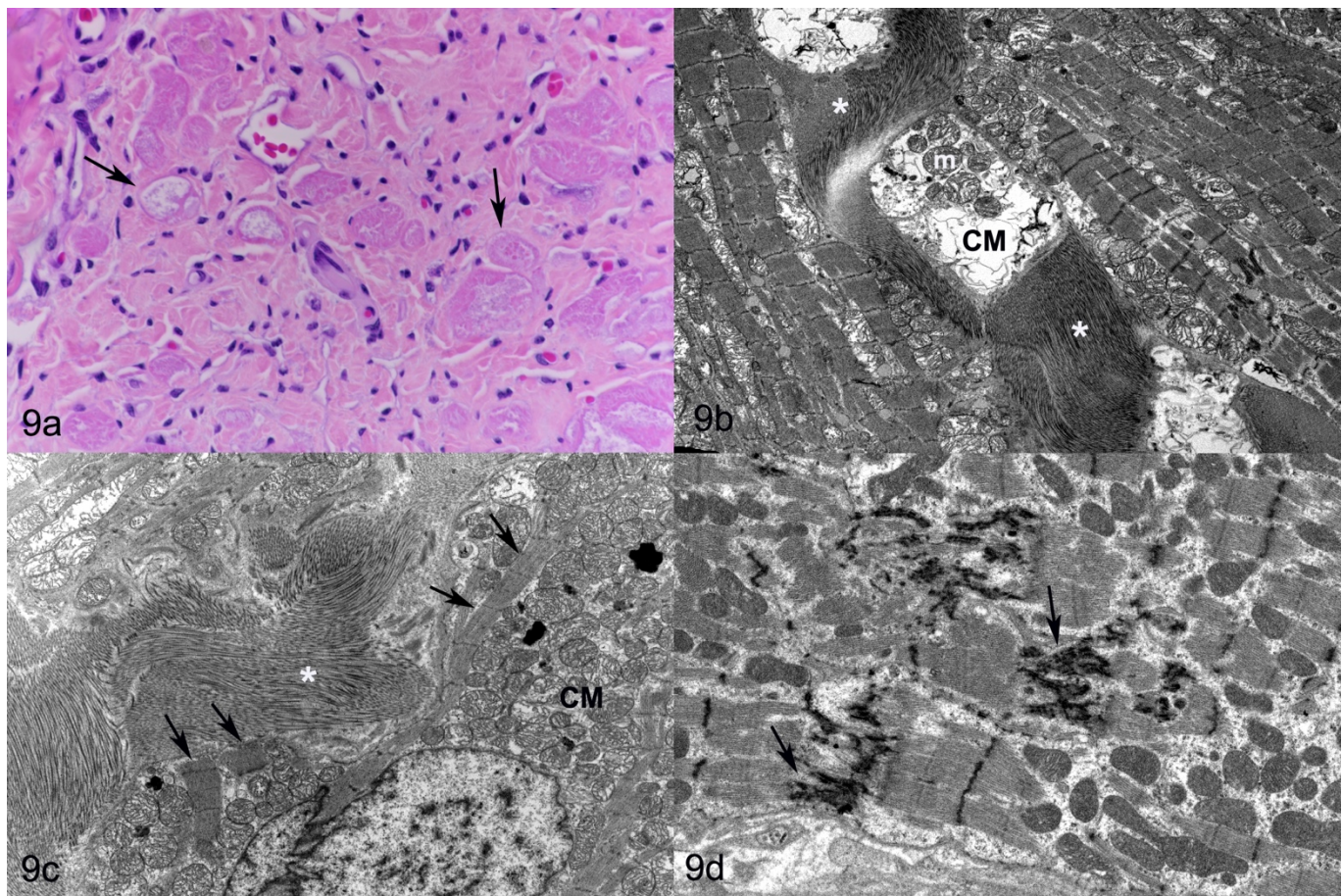


**Figure 9.** Hypertrophic cardiomyopathy (HCM), myocardium, cat, case no 1.9. Focal lesions. (a) Individual cardiomyocytes in the periphery, embedded into collagen fibers, display degenerative changes, i.e. shrinkage, loss of striation, hypereosinophilia, cytoplasmic vacuolization and fragmentation (arrows). HE stain. (b-d) Ultrastructural features. (b) Cardiomyocyte (CM) with cytoplasmic vacuolization and mitochondrial (m) swelling, surrounded by mature collagen fibers (asterisks). (c) Cardiomyocyte (CM) with thin, irregularly arranged myofibrils (arrows), embedded and walled off by dense and partially irregularly arranged mature collagen fiber bundles (asterisk). (d) Cardiomyocytes showing features of degeneration, such as myofiber disarray and disruption of intercalated disc with marked disorganisation and interdigitation of Z-lines (arrows). Transmission electron microscopy.

## Curriculum Vitae

Vorname Name	Sarah Verena Kitz
Geburtsdatum	28/01/1989
Geburtsort	Wien
Nationalität	Österreich

### Schul Ausbildung

09/1995-07/2000	Volksschule Gilgegasse 12, Wien, Österreich
09/2000 – 07/2007	RG/WRG 8 Feldgasse Bundesrealgymnasium und Wirtschaftskundliches Realgymnasium, Wien, Österreich

### Höchster Schulabschluss

07/2007	Matura, RG/WRG 8 Feldgasse Bundesrealgymnasium und Wirtschaftskundliches Realgymnasium, Wien, Österreich
---------	--

### Studium

10/2008 – 12/2014	Veterinärmedizin, Veterinärmedizinische Universität Wien, Wien, Österreich
23/12/2014	Abschlussprüfung vet.med. Veterinärmedizinische Universität Wien, Wien, Österreich
03/2015 – 08/2018	Anfertigung der Dissertation unter der Leitung von Prof. Dr.med.vet. Anja Kipar am Institut für Veterinärpathologie der Vetsuisse-Fakultät, Universität Zürich Direktorin Prof. Dr. Anja Kipar

### Fachrelevante Anstellungen nach Abschluss des veterinärmedizinischen Studiums

Seit 02/2016	Residency in Veterinärpathologie am Institut für Veterinärpathologie, Vetsuisse-Fakultät, Universität Zürich
08/2018	Externship, Bristol Veterinary School, University of Bristol, UK
03/2015-02/2016	Internship in Veterinärpathologie am Institut für Veterinärpathologie, Vetsuisse-Fakultät, Universität Zürich
Seit 03/2015	Doktorandin am Institut für Veterinärpathologie, Vetsuisse-Fakultät, Universität Zürich